Detailed investigation of the magnetic phase diagram of CeRu$_2$Ge$_2$ up to 11 GPa

H. Wilhelm, K. Alami-Yadri, B. Revaz, and D. Jaccard

Département de Physique de la Matière Condensée, Université de Genève, 24, Quai Ernest-Ansermet, CH-1211 Geneva 4, Switzerland

The electrical resistivity $\rho(T)$ and transverse magnetoresistivity of magnetically ordered CeRu$_2$Ge$_2$ (T_N = 8.55 K and T_C = 7.40 K) was measured as a function of pressure up to P = 11 GPa and down to T = 30 mK. Pressure first increases T_N and suppresses T_C. Then a second transition, corresponding probably to a modification of the AFM state, appears at $T_L < T_N$ in the pressure range $3.5 < P < 7.2$ GPa. The long-range magnetic order disappears at a critical pressure P_c = 8.7 GPa like $T_N \propto (P_c - P)^m$, with m = 0.71(8). The $\rho(T)$ curves at low temperature and low pressure ($P < 7.8$ GPa) are well described by a power law $\rho(T) \propto T^n$, with exponents $n > 2$. Well above P_c, a Fermi liquid behavior (n = 2) is observed and the A coefficient of the quadratic T dependence decreases with pressure. In the pressure interval $P_c \pm 0.8$ GPa, exponents close to n = 1.5 indicate a deviation from a Fermi liquid description. The magnetoresistivity curves show different anomalies at characteristic magnetic fields B_a, B_c, and B_M. The latter occurs close to P_c and is reminiscent of the metamagneticlike field in CeRu$_2$Si$_2$. A quantitative comparison between the (T,P) data of CeRu$_2$Ge$_2$ and the (T,x) data of CeRu$_2$(Si$_{1-x}$Ge$_x$)$_2$ on the basis of the unit-cell volume as the crucial parameter shows that the same (T,V) diagram is obtained. [S0163-1829(99)05705-7]

I. INTRODUCTION

Kondo lattice compounds are strongly correlated electron systems where the $4f(5f)$ element builds a periodic lattice in a metallic environment. These materials can have different ground states depending on the competition between the Kondo coupling (T_K) and the RKKY interaction (T_{RKKY}). The two characteristic energies depend essentially on the $4f$-electron and conduction electron coupling J like $T_K \propto \exp(-1/Jn)$ and $T_{RKKY} \propto (Jn)^2$, where n is the density of states of the conduction band at the Fermi level E_F. For small J the RKKY interaction dominates ($T_{RKKY} > T_K$) and the system orders magnetically. At intermediate J, both T_{RKKY} and T_K are of comparable strength but magnetic order still occurs. As J reaches a critical value J_c the magnetic order is finally suppressed and non-Fermi-liquid (NFL) behavior is observed in several systems. Above J_c ($T_K > T_{RKKY}$) Fermi-liquid (FL) behavior, i.e., a T^2 dependence of the electrical resistivity $\rho(T)$ below a characteristic temperature is observed.

A typical example for this dependence is the heavy fermion (HF) compound CeRu$_2$Si$_2$, where $\rho(T)$ obeys a T^2 dependence below 300 mK,[1,2] with a quadratic temperature coefficient A related to the Sommerfeld coefficient γ by the universal scaling $\gamma^2 \propto A$.[3] The large coefficient of the electronic specific heat γ = 360 mJ/mol K^2 (Ref. 4) results from an enhanced quasiparticle mass which also leads to a huge, but weakly temperature dependent, Pauli susceptibility. A representative compound of a magnetically ordered system is CeRu$_2$Ge$_2$, that exhibits an incommensurate antiferromagnetic (AFM) order below T_N = 8.5 K and enters a ferromagnetic (FM) ground state at T_C = 7.4 K.[5] At these temperatures specific heat and resistivity measurements already showed anomalies.[6,7] The Sommerfeld coefficient γ = 20 mJ/mol K^2 (Refs. 8 and 9) is small compared to that of CeRu$_2$Si$_2$ but still three times as high as that of the nonmagnetic La counterpart.[10]

The particular interest in the CeRu$_2$Si$_2$ and CeRu$_2$Ge$_2$ compounds is the possibility to study the transition from the nonmagnetic to the magnetic state. In these studies pressure is an indispensable tool. It can be achieved either by partial substitution of Ce by La or replacing Si by Ge in CeRu$_2$Si$_2$ (chemical pressure) as well as applying external pressure on CeRu$_2$Ge$_2$. The short-range AFM correlations found in CeRu$_2$Si$_2$ at low temperature[11] can either be destroyed by a magnetic field $B_M \approx 8$ T, corresponding to a metamagneticlike transition in the magnetization[4,12] or by alloying. A long-range AFM ground state is observed in Ce$_{1-z}$La$_z$Ru$_2$Si$_2$ and CeRu$_2$(Si$_{1-x}$Ge$_x$)$_2$ alloys. The critical concentration above which this ground state exists is now well defined for the first system, $z_c \approx 0.075$,[13] but for the latter x_c is less well known. From the results reported in Refs. 14 and 15 $x_c \approx 0.05 - 0.07$ can be estimated. The magnetic order was studied in detail in these solid solutions. For both La and Ge doping, neutron diffraction experiments have shown that the AFM structure is incommensurate, with a wave vector identical to one of the wave vector characterizing the AFM correlations in CeRu$_2$Si$_2$.[16,17] For La doping this ground state exists up to z = 0.2.[18] However, for a Ge content $x \gtrsim 0.7$, a FM ground state replaces the initial AFM order at low temperature.[14,15]

The substitution experiments are striking examples how the physical properties of a HF compound can be changed by expanding the unit-cell volume. Reducing the volume of CeRu$_2$Ge$_2$ by applying external pressure gives an unique opportunity to study the evolution of the FL state, seen in the CeRu$_2$(Si,Ge)$_2$ system, within one experiment on a single compound. Recent results[7,19,20] showed indeed that in CeRu$_2$Ge$_2$ the nonmagnetic ground state, with a quadratic temperature dependence of $\rho(T)$, is entered at high pressure. Here we present a detailed study of the magnetic phase diagram of CeRu$_2$Ge$_2$ by electrical resistivity and transverse magnetoresistivity (MR) measurements at high pressure ($P \leq 10.8$ GPa).

　　　　　　PRB **59**　　3651

This article is organized as follows. In Sec. II the sample preparation and the high pressure technique are reported. The ambient pressure properties of CeRu$_2$Ge$_2$, examined by specific heat, electrical resistivity and thermoelectrical power are presented in Sec. III A. Then the electrical resistivity (Sec. III B) and the MR data (Sec. III C) at high pressure are described. In Sec. IV the results are compared to those of the solid-solution CeRu$_2$(Si$_{1-x}$Ge$_x$)$_2$ and the evolution of the differently ordered magnetic phases as well as the deviation from a Fermi-liquid behavior near the magnetic to nonmagnetic transition are discussed.

II. EXPERIMENTAL DETAILS

The sample was prepared by melting stoichiometric amounts of Ce(4N), Ru(4N), and Ge(5N) in an arc furnace under argon atmosphere. The sample was melted several times to achieve good homogeneity and was annealed at 800 °C for ten days. X-ray diffraction analysis showed a good sample quality and gave $a = 4.268$ Å and $c = 10.048$ Å as lattice parameters for the ThCr$_2$Si$_2$ structure ($I4/mmm$). The ignots cleave easily in thin sheets parallel to the basal plane of the tetragonal structure. These sheets had only to be cut along the edges to obtain rectangular shaped samples for the resistivity measurements. The sample investigated at high pressure was cut from the piece used in the specific heat experiment and had a cross section of 16×122 μm^2 and a length of $l = 880$ μm.

The high pressure device used is derived from the Bridgman technique. The force applied to the nonmagnetic tungsten-carbide anvils ($\phi = 3.5$ mm) at room temperature is kept constant upon cooling by balancing the different thermal contractions of the materials used. The pressure cell is formed by a pyrophyllite gasket (internal diameter of 1.9 mm) and two steatite disks were used as pressure transmitting medium. The steatite ensures quasi-hydrostatic conditions in the pressure range explored here. The pressure gauge and sample were centered parallel to each other between the two steatite disks. The gauge is a thin Pb foil and its superconducting transition temperature yields the pressure in the sample chamber.[21] Across the gasket eight electrical leads are wedged in small gorges. This ensures electrical insulation and avoids wire breaking. The anvils used and the maximum applicable force limited the experiment to a pressure of $P \approx 11$ GPa.

The electrical resistance was obtained by the four-point method (1 μA$ < I < 1$ mA, $\vec{j} \perp \vec{c}$). The voltage was measured for opposite current directions to cancel out thermoelectrical voltages. Along the sample two voltages, V_1 and V_2 were measured between points separated by $l_1 = 190$ μm and $l_2 = 330$ μm, respectively. This makes it possible to test the homogeneity of the sample. On the Pb foil also two voltages at points opposite to those on the sample were recorded to test the pressure homogeneity. This gave pressures P_i, corresponding to each voltage V_i ($i = 1, 2$) on the sample. Below $P \approx 4$ GPa $P_1 = P_2$ was found. However, at higher pressure two different values P_i were observed. This shows the evolution of a pressure gradient which was estimated to be 0.7 GPa at $P = 10.8$ GPa. The accuracy of P_i was limited by the width of the superconducting transition in Pb of $\Delta T = 100$ mK (at 10.8 GPa), corresponding to an uncertainty of
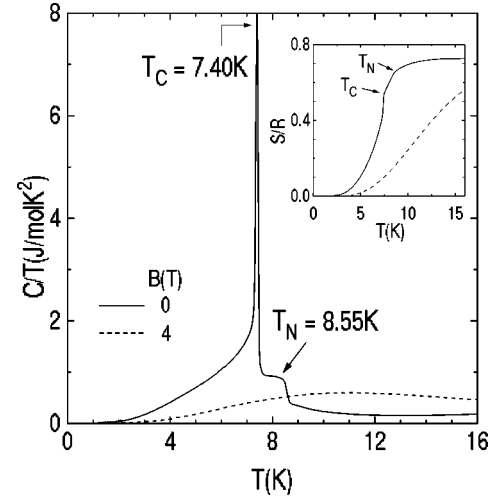
FIG. 1. Low temperature C/T of CeRu$_2$Ge$_2$ in zero field as well as in $B = 4$ T. The arrows indicate the two transition temperatures. At $B = 4$ T only one transition is seen. In the inset the magnetic entropy S/R for both magnetic fields is depicted. It was obtained by subtracting an electronic γT and phononic BT^3 contribution.

$\pm$ 0.2 GPa, much lower than the pressure gradient.

The anvils are enclosed by copper rings to ensure good thermalization of the sample.[22] Thermometers attached on one of these rings were used to determine the sample's temperature. The thermometers used were Pt for $T > 50$ K, Ge for $1.2 < T < 50$ K and RuO$_2$ for $T < 4.2$ K. The very low magnetization of the whole device allows to measure the transverse MR ($\vec{j} \perp \vec{c}$, $\vec{B} \| \vec{c}$) up to $B = 8$ T.

The setup of the thermoelectrical power (TEP) performed in the temperature range $1.2 < T < 300$ K at ambient pressure is described in Ref. 23. The specific heat was measured with a method derived from a relaxation technique.[24]

III. RESULTS

A. Ambient pressure properties

The two magnetic phase transitions in CeRu$_2$Ge$_2$ are clearly visible in the specific heat as can be seen in Fig. 1. In zero magnetic field a relatively small step ($C/T = 2$ J/mol K^2) occurs at $T_N = 8.55$ K whereas a huge peak ($C/T = 8$ J/mol K^2) is visible at $T_C = 7.40$ K. The sharpness of the peak at T_C cannot be explained by a second order phase transition as was proposed in Ref. 8. The specific heat at low temperature can be written as

$$C_{tot} = C_{el} + C_{ph} + C_m, \tag{1}$$

with $C_{el} = \gamma T$ the electronic, $C_{ph} = BT^3$ the phononic, and C_m the magnetic part of the specific heat. The latter contribution takes a gap Δ in a FM spin wave excitation spectrum into account and is given by[25]

$$C_m = \beta(\Delta^2/\sqrt{T} + 3\Delta\sqrt{T} + 5\sqrt{T^3})\exp(-\Delta/T), \tag{2}$$

with a constant β. This equation was derived for the simple rare earth metals. The data below $T = 5.5$ K are very well described by this formula. Small corrections in Eq. (2) might be possible due to the different crystal structure of the rare
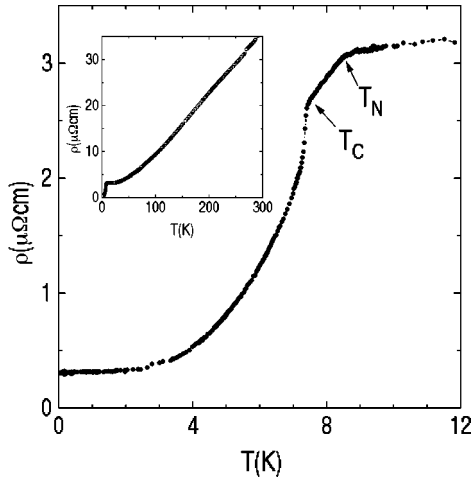
FIG. 2. Low temperature variation of $\rho(T)$ of CeRu$_2$Ge$_2$ at ambient pressure. At T_N and T_C the magnetic phase transitions occur. The entire temperature range is shown in the inset.

FIG. 3. The thermoelectrical power $S(T)$ of CeRu$_2$Ge$_2$ at ambient pressure. The arrows mark the magnetic transition temperatures $T_N = 8.55$ K and $T_C = 7.40$ K.

earth metals and CeRu$_2$Ge$_2$. The Sommerfeld coefficient $\gamma = 19.3$ mJ/mol K^2 is in agreement with that reported in Refs. 8 and 9 and the FM gap and the Debye temperature are estimated to $\Delta = 14.1$ K and $\Theta_D = 260$ K, respectively. If only the third term in Eq. (2) is used, as was done in Refs. 8 and 9, a slightly lower gap value ($\Delta \approx 10$ K) is obtained but the other quantities are unchanged.

The entropy gain connected with the magnetic transitions reaches $S/R = 0.72$ (see inset Fig. 1), close to the theoretical value $S/R = \ln 2 = 0.69$, expected for $S = 1/2$ spin magnetism. It is noted that the former S/R value is found in literature[6,8,9,26] regardless of the height of the FM peak and the occurrence of the AFM order.

A magnetic field applied along the c-axis has a rather strong influence on the transitions. A field as small as $B = 0.05$ T shifts T_N to lower temperatures and decreases the height of the peak at T_C by a factor of 2. At $B = 0.1$ T, T_N has decreased further but T_C is still at the same temperature as in zero field. Both peaks seem to have merged into a single feature at $B = 0.15$ T.[27] The maximum at the AFM to FM transition (clearly evident at $B < 0.05$ T) vanished at higher fields as is shown for $B = 4$ T in Fig. 1.

The two magnetic transitions are also clearly visible in the electrical resistivity as is shown in Fig. 2. The change of slope in $\rho(T)$ at $T_N = 8.55$ K and $T_C = 7.40$ K are well distinguished in comparison to what was found in Ref. 28.

Assuming that a FM gap exists in the magnon excitation spectrum, as mentioned above, the low temperature resistivity can be described by[25]

$$\rho(T) = \rho_0 + AT^2 + BT^2 \exp(-\Delta/T), \qquad (3)$$

where the first term describes the imperfection scattering, the second part accounts for electron-electron or electron-magnon scattering, and the exponential term corresponds to the contribution of an anisotropic ferromagnet with a gap Δ in the spin wave spectrum. Below 5 K the $\rho(T)$ curve at ambient pressure is well described by this equation and the fit yields $A = 4 \times 10^{-3}$ $\mu\Omega$ cm/K^2, $B = 0.1$ $\mu\Omega$ cm/K^2 and $\Delta = 11$ K. Using the empirical relation between A, accounting for electron-electron scattering, and γ
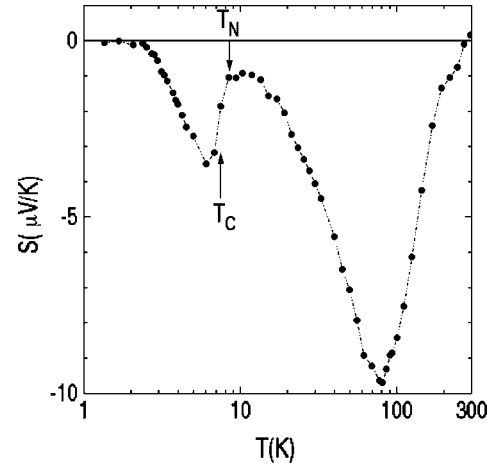
$$A = 10^{-5} \times \gamma^2, \qquad (4)$$

found for several Ce and U compounds,[3] a Sommerfeld coefficient of the specific heat $\gamma = 20$ mJ/mol K^2 is derived in excellent agreement with the value reported above. No anomaly in the high temperature part of $\rho(T)$ is seen and $\rho(T)$ follows a linear temperature dependence between $T \approx 100$ K and 300 K (see inset, Fig. 2).

The resistivity of CeRu$_2$Ge$_2$ at ambient pressure is smaller along the c axis than perpendicular to it.[29] The ratio $\rho_{\perp c}/\rho_{\parallel c} \approx 1.5$ is almost temperature independent down to 1.2 K, the lowest temperature measured. This ratio is comparable to that of CeRu$_2$Si$_2$.[30]

The difference between CeRu$_2$Si$_2$ and CeRu$_2$Ge$_2$ becomes evident in the thermoelectrical power $S(T)$. In the former compound a broad maximum is centered around 220 K whereas $S(T)$ of the latter is always negative for $T < 290$ K (see Fig. 3). The most striking features in $S(T)$ of CeRu$_2$Ge$_2$ are the minima present at $T_{min,S}^{(1)} = 80$ K and $T_{min,S}^{(2)} = 6$ K, with $S = -9.7$ μV/K and -3.5 μV/K, respectively. Comparing this temperature dependence to that reported for other magnetic Ce compounds, e.g., CePd$_2$Si$_2$ (Ref. 31) and CeCu$_2$Ge$_2$ (Ref. 32) reveals a clear difference. The latter compound shows a positive bump at high temperature like CeRu$_2$Si$_2$ followed by a negative minimum around 20 K. A second positive peak in $S(T)$ develops at lower temperature and a sign change occurs around $T_0 = 50$ K. The high temperature maximum was attributed to the interplay of the Kondo effect and the crystal field (CF) effect while the negative values of $S(T)$ were assigned to spin interactions. The absence of a positive contribution at high temperature in $S(T)$ of CeRu$_2$Ge$_2$ can be attributed to the fact that CF effects play a minor role because both, $\Delta_{CF}^{(1)} = 500$ K and $\Delta_{CF}^{(2)} = 750$ K (Refs. 26 and 33) are well above room temperature and T_K is assumed to be very small.[34] The appearance of a minimum in $S(T)$ at $T_{min,S}^{(1)}$ seems to be too high in temperature to be explained by spin interactions. The
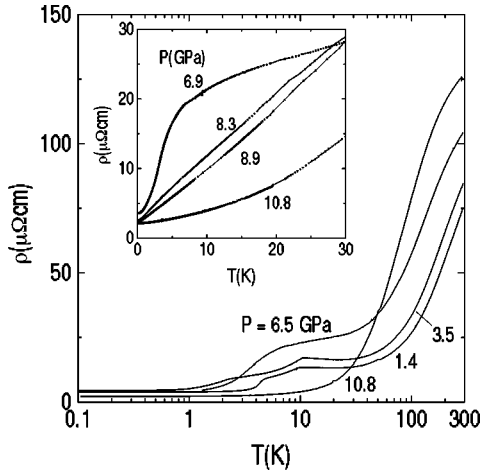
FIG. 4. Temperature dependence of the electrical resistivity of $CeRu_2Ge_2$ at selected pressures. In the inset the change of the curvature at low temperature around the critical pressure P_c $= 8.7$ GPa is shown.

anomaly around $T_{min,S}^{(2)}$ is interpreted as a sign for the opening of a gap, in good agreement with the findings of the specific heat and electrical resistivity, reported in the first part of this section.

B. Electrical resistivity at high pressure

Representative $\rho(T)$ curves of $CeRu_2Ge_2$ at high pressure are shown in Fig. 4 in a semi-logarithmic plot. At low temperature a weakly pressure dependent residual resistivity ($\rho_0 \approx 3$ $\mu\Omega$ cm) is observed. The room temperature $\rho(T)$ values increase continuously from $\rho \approx 75$ $\mu\Omega$ cm (P $= 0.5$ GPa) up to $\rho \approx 130$ $\mu\Omega$ cm at $P = 10.8$ GPa. This might be a precursor of a high-temperature maximum. The signs of magnetic order are clearly visible in the temperature range 1 K $< T < 10$ K. Across the transitions $\rho(T)$ drops by more than 80%. This large drop is an additional indication of the high quality of the sample. The magnetic order disappears in the pressure range 6.9 GPa $< P < 10.8$ GPa (see inset Fig. 4). Before the typical quadratic temperature dependence of a nonmagnetic system is reached (curve recorded at 10.8 GPa) the $\rho(T)$ curves seem to show an unusual linear temperature dependence up to ≈ 30 K in a small pressure interval. The $\rho(T)$ dependence of these curves at low temperature ($T \lesssim 1.5$ K) will be examined in detail further below.

The transition temperatures were extracted from the $\rho(T)$ curves using the change of slope in the temperature derivative of $\rho(T)$ and their pressure dependence is plotted in Fig. 5. The AFM transition first increases with an initial slope $\partial T_N / \partial P = 0.7$ K/GPa, reaches a maximum of 10.7 K at P $= 4.1$ GPa and finally decreases. The extrapolation T_N $\propto (P_c - P)^m \to 0$, made for $P \geqslant 6.0$ GPa, leads to a critical pressure $P_c = 8.70(5)$ GPa and $m = 0.71(8)$. The FM transition temperature decreases ($\partial T_C / \partial P = -2.1$ K/GPa) in the pressure range up to $P = 2.7$ GPa. Above P $= 3.5$ GPa, $CeRu_2Ge_2$ seems to be in a different magnetically ordered ground state. The low temperature transition at $P = 3.5$ GPa has become broader while the transition at T_N is as clear as at $P = 1.4$ GPa (see Fig. 4). Therefore, a tran-
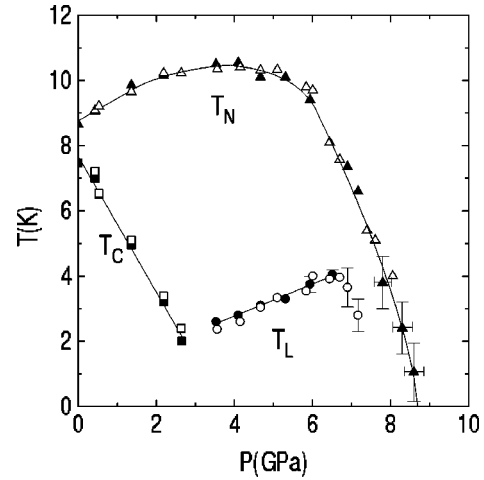
FIG. 5. (T, P) phase diagram of the transition temperatures in $CeRu_2Ge_2$. T_C is suppressed at low P and a new transition appears at T_L. T_N vanishes at $P_c = 8.7$ GPa. The open and bold symbols distinguish the transition temperatures obtained at two parts of the sample (see Sec. II).

sition temperature T_L, labeled in analogy to $Ce_{0.8}La_{0.2}Ru_2Si_2$ and $CeRu_2(Si_{0.9}Ge_{0.1})_2$,[16] is introduced as it was done in Refs. 7 and 19. It increases slightly with pressure ($\partial T_L / \partial P$ $= 0.5$ K/GPa) and is not visible anymore beyond P $= 7.2$ GPa. Above $P = 6.5$ GPa, the determination of the transition temperatures became difficult because of the large transition width (see, e.g., curve at $P = 6.9$ GPa in the inset of Fig. 4). This is taken into account by the error bars in Fig. 5.

The $T_N(P)$ variation can be compared qualitatively with the Doniach description,[35] which reflects the competition between the Kondo effect $T_K \propto \exp(-1/Jn(E_F))$ and the RKKY interaction $T_{RKKY} \propto (Jn(E_F))^2$. For small $Jn(E_F)$ values, the latter dominates the Kondo effect, as in $CeRu_2Ge_2$ at low pressure. As pressure favors the increase of $Jn(E_F)$, the system is forced towards the nonmagnetic phase. The competition between T_K and T_{RKKY} was also used by Borges and co-workers[36] to explain the pressure effect on the ordering temperature of some $CeRu_2(Si_{1-x}Ge_x)_2$ compounds.

The low temperature part of the $\rho(T)$ curves measured up to $P = 2.7$ GPa is well described with Eq. (3). Pressure induces a decrease of the gap to $\Delta = 1.5$ K at $P = 2.7$ GPa. Assuming, that at T_L the magnetic order becomes AFM, the exponential part of Eq. (3) has to be replaced by

$$\rho_m = \widetilde{B}T(1 + 2T/\Delta)\exp(-\Delta/T), \qquad (5)$$

proposed for AFM spin-wave excitations.[37] Here $\widetilde{B}$ is a constant. With this magnetic contribution the $\rho(T)$ data are well described for $T < 3$ K and up to 6 GPa. A weak increase of the gap ($\Delta = 2.3$ K at 6 GPa) is observed.

As was pointed out in Ref. 25, it is difficult to distinguish an exponential temperature dependence of $\rho(T)$ from a power law $\rho(T) \propto T^4$ at temperatures lower than the gap temperature. The latter behavior corresponds to a linear dispersion relation of FM spin waves. To take a power law behavior of the electrical resistivity into consideration, the $\rho(T)$ curves were described below $T_A = 1.5$ K according to
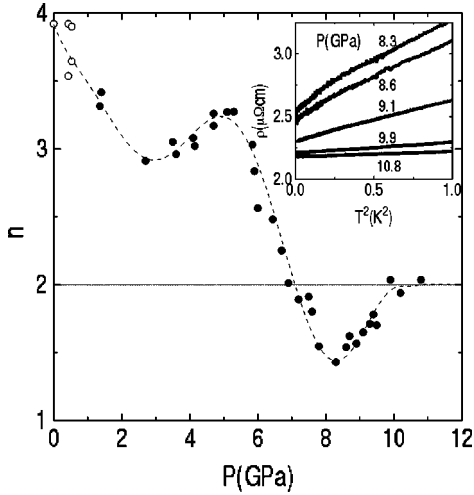
FIG. 6. Pressure variation of the exponent n used in the power law of Eq. (6) to describe the $\rho(T)$ data of $CeRu_2Ge_2$ below $T = 1.5$ K. The temperature interval had to be enlarged up to 4 K for $P < 1$ GPa. In the inset $\rho(T) \propto T^2$ below 1 K is plotted.

$$\rho = \rho_0 + \tilde{A}T^n, \qquad (6)$$

with an exponent n and a coefficient $\tilde{A}$ as fitting parameters. The result of this procedure is shown in Fig. 6, where n is plotted versus pressure. The exponent decreases from $n \approx 4$ at low pressure to $n \approx 3$ at $P = 2.7$ GPa. The variation of n starting at 3.5 GPa is interpreted as a sign of a change in the magnetic ordering. The exponent decreases down to $n = 2$ around 7 GPa, which seems to coincide with the pressure where T_L was not seen anymore (see Fig. 5). Then a rather large pressure interval around P_c exists ($7.8 \leq P \leq 9.5$ GPa) where n attains values between $3/2 \leq n \leq 5/3$. The two extreme values are predicted for AFM (Ref. 38) and FM (Ref. 39) spin fluctuations, respectively. Several $\rho(T)$ curves are plotted versus T^2 below 1 K in the inset of Fig. 6 and the deviation from a T^2-dependence is obvious. At pressures higher than 9.5 GPa the $\rho(T)$ curves show a T^2 dependence (curves recorded at $P = 9.9$ and 10.8 GPa). Thus the FL region is entered.

Close to the critical pressure the exponent shows a clear deviation from a FL behavior ($n = 2$) and this is explicitly shown in Fig. 7 for a $\rho(T)$ curve measured just above P_c. In this figure the $\rho(T)$ curve recorded at 8.9 GPa is plotted versus $T^{1.57}$. The straight line indicates that this temperature dependence is appropriate between 30 mK $< T < 1.5$ K. As already mentioned above, a linear temperature dependence in the T range 1.5 K $< T < 10$ K is found (see inset, Fig. 7).

These considerations show the importance of the analysis of the low temperature data ($T < 1.5$ K) in the vicinity of P_c and how the deduced $\rho(T)$ behavior, either a power law or a linear temperature dependence, dependent on the temperature interval considered. However, the temperature dependence $\rho(T) = \rho_0 + AT^2$ was also fitted to the data below a pressure dependent temperature T_A to extract the A coefficient and to check if T_A is pressure enhanced. It is emphasized that these fits described the data (for $P < 9.5$ GPa) not as good as the fits according to Eq. (6). However, it is found that T_A is very low ($T_A < 500$ mK) for $7 < P < P_c$ and starts
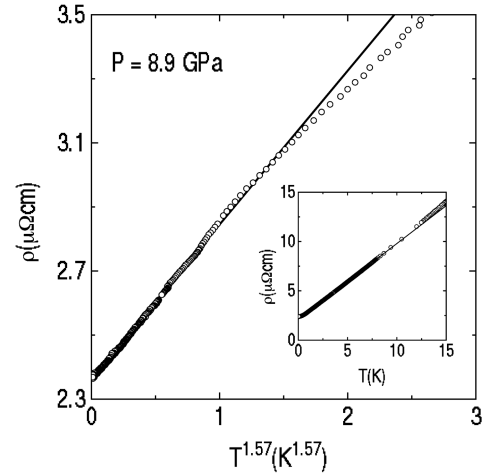
FIG. 7. Electrical resistivity $\rho(T) \propto T^{1.57}$ of $CeRu_2Ge_2$ at $P = 8.9$ GPa. A linear variation of $\rho(T)$ is found between 1.5 K $< T < 10$ K, as shown in the inset.

to increase just above P_c, reaching ≈ 2 K at 10.8 GPa. The pressure variation of the A coefficient is plotted in Fig. 8. In the pressure range $P_c < P \leq 10.8$ GPa, A decreases by one order of magnitude to a value $A = 0.04$ $\mu\Omega$ cm/K^2. To compare these results with those of $CeRu_2Si_2$, the pressure variation of $1/\sqrt{A}$ is presented in the inset of Fig. 8 together with the data reported for $CeRu_2Si_2$.[1,40–42] The $1/\sqrt{A(P)}$ behavior in the nonmagnetic phase resembles qualitatively that of $CeRu_2Si_2$, if for the latter a pressure shift of 9.1 GPa is assumed. However, the difference in absolute values of $1/\sqrt{A(P)}$ remains to be resolved.

C. Magnetoresistivity at high pressure

In the preceding section evidence of a pressure induced magnetic to nonmagnetic transition was found at P_c. Furthermore, a change of the ground state magnetic properties is very likely to happen around 3.5 GPa. These findings are supported by transverse MR measurements ($\vec{B} \| \vec{c}$ and $\vec{j} \perp \vec{c}$)
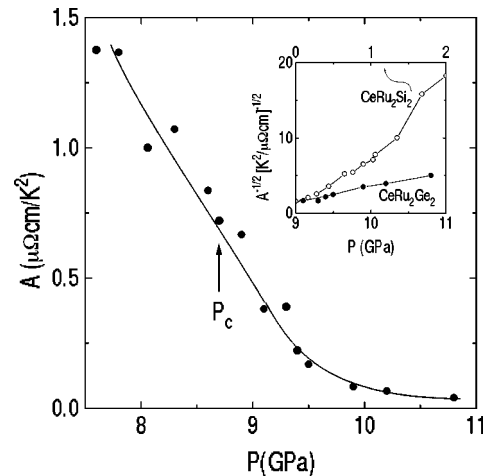
FIG. 8. A coefficient of the quadratic temperature dependence ($n = 2$ fixed) of $\rho(T)$ in $CeRu_2Ge_2$. In the inset a comparison of $1/\sqrt{A}$ for both $CeRu_2Ge_2$ and $CeRu_2Si_2$ is shown. For the latter the upper pressure axis has to be used.
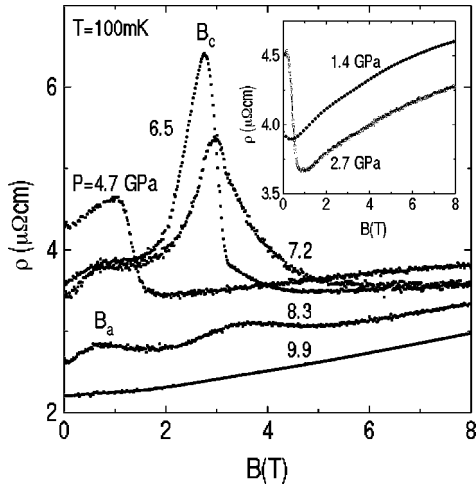
FIG. 9. Magnetoresistivity of $CeRu_2Ge_2$ at $T = 100$ mK for different pressures. In the inset the MR at low pressure is shown.

FIG. 10. (B,P) phase diagram of $CeRu_2Ge_2$ at $T = 100$ mK. The critical fields B_a and B_c are defined in analogy to the $(Ce,La)Ru_2Si_2$ system (Ref. 16).

performed for almost all pressures at several temperatures. For some particular pressures, the $\rho(T)$ curves were recorded in selected magnetic fields ($B \leqslant 8$ T). Figure 9 shows the MR measured at $T = 100$ mK at various pressures. A peak at $B \approx 1$ T is found in the MR at $P = 4.7$ GPa. It becomes a pronounced feature at 6.5 GPa and a shoulder remains at $B \approx 1$ T. The MR curves are without any anomaly above 9 GPa. The features in $\rho(B)$ above 4.7 GPa seem to have developed gradually. The low pressure MR curve at 2.7 GPa (inset of Fig. 9) shows a pronounced minimum at $B \approx 1$ T, which seems to exist already at 1.4 GPa. In both cases an increase of almost 20% follows up to $B = 8$ T. The curvature of $\rho(B)$ in the FM phase suggests, that the MR attains a maximum well above 8 T. In the curves recorded above $P = 4.7$ GPa this is not the case and the pronounced features seem to be superimposed to an always positive MR as observed in the nonmagnetic phase (+50% at $B = 8$ T at $P = 9.9$ GPa). The peaks occur at critical magnetic fields B_a and B_c, labeled in analogy to $Ce_{1-z}La_zRu_2Si_2$ and $CeRu_2(Si_{0.9}Ge_{0.1})_2$.[43–45] Details on the magnetic order at this fields will be given in Sec. IV.

The pressure dependence of B_a and B_c is plotted in the (B,P) diagram shown in Fig. 10. The lower critical field $B_a \approx 0.9$ T is rather pressure independent whereas B_c increases strongly from 1 T to 4 T in the pressure range 4 GPa $< P < 9$ GPa. This agrees very well with the (B,P) diagram found for $CeRu_2(Si_{0.9}Ge_{0.1})_2$ (Ref. 45) and supports the assignment of the maximum in $\rho(B)$ as B_a and B_c, respectively.

Figure 11 shows the field dependence of the relative MR, $\Delta\rho/\rho = (\rho(B) - \rho(0))/\rho(0)$ at $P = 7.8$ GPa for various temperatures. At low temperature ($T < 1$ K) two broad maxima corresponding to B_a and B_c are found. No signs of these fields are seen at $T = 1$ K and 6 K, respectively. However, a broad maximum in the MR is found above $T = 1$ K at $B_M \approx 4.7$ T, reminiscent of the metamagneticlike field in $CeRu_2Si_2$.[12,46] The MR measured at $T = 4.2$ K shows that $B_M \approx 5$ T (at $P = 7.8$ GPa) increases up to $B_M \approx 8$ T at $P = 8.6$ GPa. At higher pressure no indication of B_M is found below 8 T, the highest field accessible in this experiment. As already mentioned above, these features are superimposed on
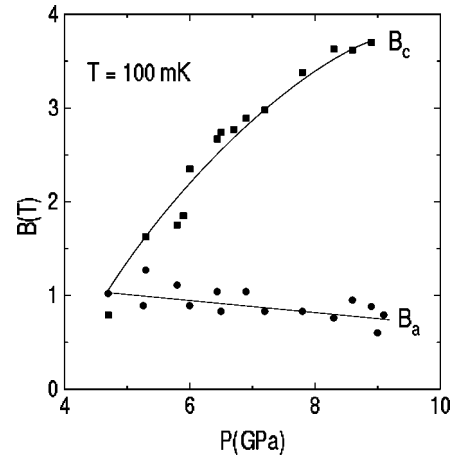
an always positive MR. In contrast to this, an always negative MR was found in the magnetically ordered $(Ce,La)Ru_2Si_2$ alloys[47] and in other MR measurements of $CeRu_2Ge_2$ under pressure performed at 1.3 K.[19,20] These different $\rho(B)$ dependencies are probably related to the large zero-field values, which are roughly one order of magnitude higher than those measured in the present experiment ($\rho \approx 3$ $\mu\Omega$ cm).

The magnetic field values where the maxima in $\rho(B)$ occur is plotted in the (B,T) phase diagram in Fig. 12. The lower critical field B_a was only seen below 1 K and therefore a phase line according to that observed in $CeRu_2(Si_{0.9}Ge_{0.1})_2$ is assumed. The higher critical field B_c found at 7.8 GPa as well as 6.5 GPa is close to the value found for $CeRu_2(Si_{0.9}Ge_{0.1})_2$.[45] In the latter compound no signs of another phase line above B_c were detected. The metamagnetic like transition occurring in the magnetization of $CeRu_2Si_2$ is also observed in ordered $Ce_{1-z}La_zRu_2Si_2$ for $z \lesssim 0.13$.[4] Below T_N, two metamagnetic steps corresponding to B_a (transition from one AFM phase to an other) and B_c (entrance in the polarized state) are seen, while B_M occurs just above B_c.
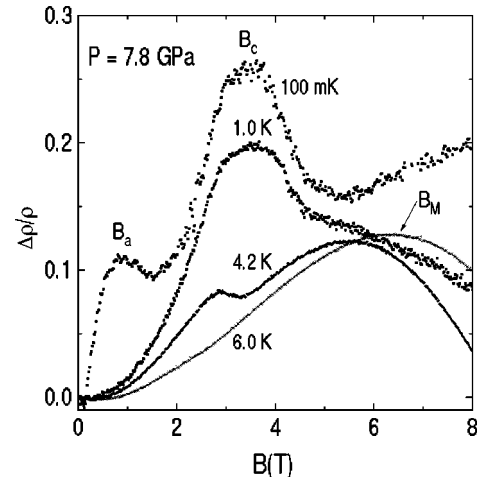
FIG. 11. Relative magnetoresistivity $\Delta\rho/\rho$ of $CeRu_2Ge_2$ at 7.8 GPa at different temperatures [with $\rho(B=0) \approx 3$ $\mu\Omega$ cm]. Three characteristic fields B_a, B_c, and B_M are observed.
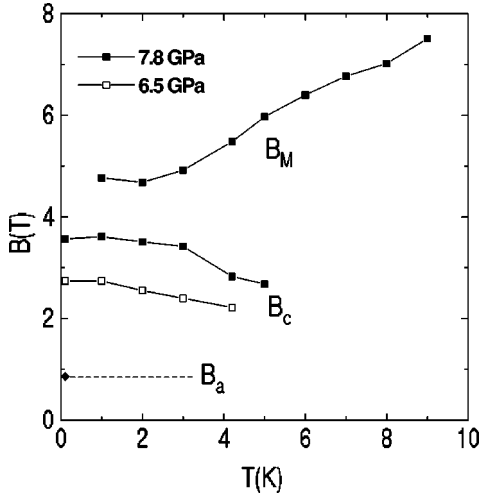
FIG. 12. (B,T) phase diagram of CeRu$_2$Ge$_2$ at 7.8 GPa (bold symbols) and 6.5 GPa (open symbols). For both pressures, B_a is the same. No signs of B_M were seen in the MR at 6.5 GPa.

In the magnetoresistivity B_a leads to a small anomaly, while a large drop occurs at B_c. However, B_M is hardly seen.[47] Thus, the occurrence of B_M in CeRu$_2$Ge$_2$ at $P = 7.8$ GPa might be correlated with the vicinity of the magnetic instability. This point is supported by the (B,T) diagram obtained for $P = 6.5$ GPa where only B_c and B_a are present.

The field dependence of the A coefficient can be deduced from $\rho(T)$ measurements in different magnetic fields, performed in the pressure range 6.0 GPa $< P <$ 7.8 GPa (Fig. 13). This $A(B)$ behavior can provide a deeper insight into the magnetic ordering just below P_c. A maximum occurs in $A(B)$ around $B \approx 2.5$ T for $P = 6.5$ GPa and seems to be correlated to the critical field B_c (see Fig. 10). The influence of the magnetic field on $\rho(T)$ at this pressure is shown in the inset of Fig. 13. A small field (of the order of 2 T) seems to shift the magnetic order to lower temperatures. In higher field ($B = 4$ T) a quadratic temperature dependence for $\rho(T)$ with a smaller A coefficient is found. A $\rho(T)$ measurement in 2 T performed at 6.9 GPa revealed also an enhanced A
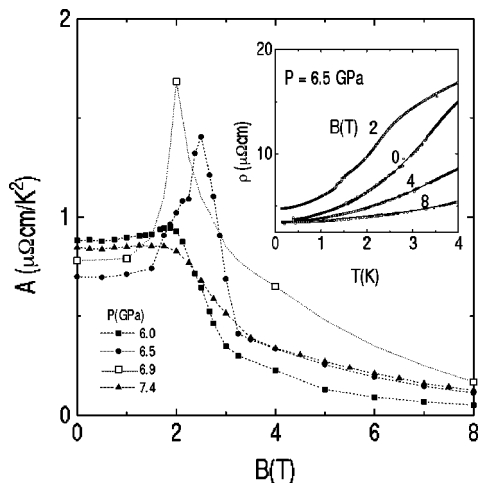
FIG. 13. Field variation of the A coefficient of the T^2 dependence of $\rho(T)$ for CeRu$_2$Ge$_2$ at different pressures. In the inset the influence of a magnetic field on $\rho(T)$ recorded at 6.5 GPa is plotted below 4.2 K.

value in respect to that obtained in other fields. No maximum in A was found at $P = 7.4$ GPa and a fit of a quadratic temperature dependence to the data recorded at $P = 7.8$ GPa was not possible.

This field dependence of A can be compared to the enhancement of the electronic specific heat coefficient γ [according to Eq. (4)] observed in Ce$_{1-z}$La$_z$Ru$_2$Si$_2$ alloys.[4] For $z = 0.13$ an AFM order is present and the increase of γ was correlated, as in the case of CeB$_6$,[48] to the existence of different magnetic structures below B_c. In contrast, for $P = 7.4$ GPa, no maximum occurs and A decreases above $B \approx 2$ T. This peculiar field dependence of A coincides with the disappearance of T_L (see Fig. 5). Thus, the $A(B)$ dependencies point to a complex magnetic order just below the critical pressure.

IV. DISCUSSION

The (T,P) diagram of CeRu$_2$Ge$_2$ presented in Fig. 5 resembles qualitatively the (T,x) diagram of CeRu$_2$(Si$_{1-x}$Ge$_x$)$_2$ where the ordering temperatures are plotted as a function of the Ge content x.[14,15] The analogy of pressure and x variation (equivalent to a chemical pressure), is supported by the appearance of the three critical magnetic fields B_a, B_c, and B_M in CeRu$_2$Ge$_2$. Thus, a quantitative comparison between CeRu$_2$Ge$_2$ and its Si substituted alloys can be made if the unit-cell volume V is taken as common variable. Both, pressure and a decrease in x correspond to a reduction in the unit-cell volume V. From x-ray diffraction studies of the alloys reported in Ref. 49 the relation $V(x) = 172.38$ Å$^3 + 10.67x$ is deduced. The volume for a given pressure applied on CeRu$_2$Ge$_2$ can be calculated with an equation of state (EOS) if the bulk modulus B_0 is known. X-ray experiments on CeCu$_2$Si$_2$ and CeRu$_2$Si$_2$ gave B_0 around 130 GPa (Refs. 50 and 51) and 122 GPa,[42] respectively. Assuming that the unit-cell volume of CeRu$_2$Ge$_2$ at P_c is the same as that of CeRu$_2$(Si$_{1-x}$Ge$_x$)$_2$ for $x = 0.05$, which seems to be very close to the critical concentration x_c, the Murnaghan EOS (Ref. 52)

$$V(P) = V_0 \left\{ \frac{B_0'}{B_0} P + 1 \right\}^{-1/B_0'}, \qquad (7)$$

with $B_0' = 4$ gives $B_0 = 135$ GPa for CeRu$_2$Ge$_2$. With the $V(x)$ and $V(P)$ relations the transition temperatures for both, CeRu$_2$(Si$_{1-x}$Ge$_x$)$_2$ and CeRu$_2$Ge$_2$ can be plotted versus the volume in the same (T,V) diagram as is shown in Fig. 14. In the case of CeRu$_2$(Si$_{1-x}$Ge$_x$)$_2$ the transition temperatures obtained by Haen and co-workers[14,15] are used. At low pressure, i.e., large V/V_0 values, the agreement is very good and in the intermediate regime the T_L values agree also except for the two values $x = 0.4$ and $x = 0.2$. Close to the magnetic instability the T_N values of the solid solution are slightly higher than those obtained in this experiment. They can be extrapolated to zero using the power law $T_N \propto (x - x_c)^{\tilde{m}}$, with $x_c = 0.096$ and $\tilde{m} = 0.13$. A comparison between the exponents m [used in $T_N \propto (P_c - P)^m$] and $\tilde{m}$ is not possible because x can not be transformed into P as $V(P)$ is a nonlinear function in P [see Eq. (7)].
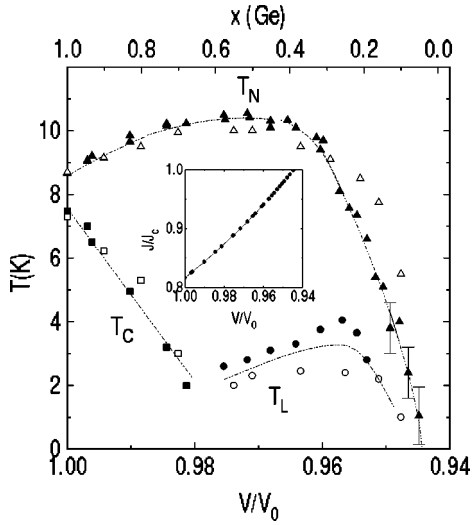
FIG. 14. Magnetic ordering temperatures plotted versus the relative unit-cell volume V/V_0 for $CeRu_2Ge_2$ (bold symbols) and the Ge content x in the solid-solution $CeRu_2(Si_{1-x}Ge_x)_2$ (open symbols) taken from Refs. 14 and 15. The volume is normalized to the value $V_0 = 183.03$ Å^3 of $CeRu_2Ge_2$ at ambient pressure.

Several regions with different magnetic ground states can be distinguished from Fig. 14. A double transition region (AFM plus FM) exists for $0.7 \leq x \leq 1.0$ (Ref. 15) or $P < 3.5$ GPa. The long-range magnetic order in the AFM phase is modulated with a wave vector $\vec{k}_1 = (0.309, 0, 0)$,[5] identical to that of the short-range magnetic correlations in $CeRu_2Si_2$.[53] In the FM phase the magnetic moment is aligned along the c-axis and has a value $\mu = 1.9\mu_B$.[5,33]

Two AFM phases seem to exist for $0.1 \leq x < 0.7$ (3.5 GPa $\leq P < 7.8$ GPa) characterized by T_L and T_N, with $T_L < T_N$. Detailed neutron studies on $CeRu_2(Si_{0.9}Ge_{0.1})_2$ (Ref. 45) revealed a complex (B, T) phase diagram. At low temperature and up to a field B_a the reflections associated with $\vec{k}_1$ are unchanged (phase I), even on crossing T_L. However, at the latter temperature some modifications in the intensity of the third harmonic of the moment modulation can occur[17] and some anomalies were observed by inelastic neutron scattering.[54–57] Above B_a, two distinct AFM phases are found, depending on temperature. In the high temperature phase (phase III) not only $\vec{k}_1$ is seen but also $\vec{k}_2 = (0.309, 0.309, 0)$ (which is the other wave vector characterizing the AFM correlations in $CeRu_2Si_2$) plus a FM component. The low temperature phase (phase II) is commensurate with $\vec{k}_3 = (1/3, 1/3, 0)$. The transition from phase III to phase II is described as a lock-in of $\vec{k}_2$ to a commensurate value.[17] Thus, it is very likely that a transition in low field ($B < B_a$) at $T_L < T_N$ occurs also in $CeRu_2Ge_2$ at intermediate pressure like in $CeRu_2(Si_{1-x}Ge_x)_2$ alloys.

In the electrical resistivity measurements only one transition is detected in the range 7.8 GPa $< P < P_c$ ($0.05 < x < 0.1$). This might point to the possibility that T_L is very close to zero. To clarify this, detailed neutron scattering experiments below 2 K have to be performed for $0.05 < x < 0.1$. No long-range magnetic order is observed above P_c, but the electrical resistivity reveals a deviation from a FL behavior in the pressure range up to 9.5 GPa (see Fig. 6).

Above this pressure, the FL region is eventually entered and the characteristic $\rho(T) \propto AT^2$ dependence is seen analogously to $CeRu_2Si_2$ as shown in the inset of Fig. 8. Unfortunately no comparison to the temperature dependence of the electrical resistivity of $CeRu_2(Si_{1-x}Ge_x)_2$ with $x = x_c$ is possible because they are not measured yet. However, in $Ce_{1-z}La_zRu_2Si_2$ with $z = z_c = 0.075$ a quadratic temperature variation of $\rho(T)$ was found in the range 30 mK $< T < 1$ K.[58]

These reflections on the (T, V) phase diagram show that the unit-cell volume and therefore interatomic distances are the crucial parameter. The changes in the interatomic distances enter in the exchange coupling J_{cf} (Ref. 59)

$$J_{df} \propto V_{cf}^2/(E_F - E_f) \tag{8}$$

via V_{cf}, the hybridization of conduction and $4f$ electrons. The hybridization can be written as[60]

$$V_{cf} \propto 1/d^{l+l'+1}, \tag{9}$$

with l and l' the angular momentum ($l, l' = 0, 1, 2, \ldots$ for s, p, d, $\ldots$, respectively) and the interatomic distance d between Ce and a ligand. The main effect arises from the f-d hybridization and therefore only the V_{df} hybridization is considered in the following. Pressure enters V_{df} via the Ce-Ru distance $d = 0.25\sqrt{4a^2 + c^2}$. To calculate the volume dependence of the lattice parameter $a(V)$ and $c(V)$ with Eq. (7), the compressibilities κ_a and κ_c of $CeRu_2Ge_2$ are deduced from $\kappa_V = 2\kappa_a + \kappa_c$ using $\kappa_a/\kappa_c = 1.35/3.15$ found for $CeRu_2Si_2$.[42] Recent photoemission data on $CeRu_2Si_2$ and $CeRu_2Ge_2$ (Ref. 61) showed similar features at almost the same energies near E_F for both compounds. Therefore it is assumed that $E_F - E_f$ hardly changes at low pressure. With these ingredients the volume dependence of the exchange interaction J can be deduced as is shown in the inset of Fig. 14. The J/J_c variation with the reduced volume V/V_0 should, in principle, allow to calculate the pressure dependence of T_K using $T_K \propto \exp(-1/Jn(E_F)) \propto 1/\sqrt{A}$. The T_K value in $CeRu_2Ge_2$ at ambient pressure is found to be 4 K which is slightly higher than that reported in Ref. 34. At P_c it reaches a value similar to that in $CeRu_2Si_2$.[10] It is mentioned that at high pressure the system approaches the intermediate valence regime and therefore $E_F - E_f$ should decrease. Thus, the J/J_c behavior would be further enhanced.

In the framework of the spin fluctuation theory,[38] predictions for the temperature dependence of $\rho(T)$ as well as the variation of the ordering temperature with pressure can be made. Moriya and Takimoto[38] showed that the spin fluctuation theory developed for itinerant d-electrons can be modified and applied to nearly localized f-electron systems. The key ingredient of this theory is the dynamical susceptibility $\chi(q, \omega)$ arising from overdamped spin fluctuation modes. Their population can be calculated quantitatively, once $\chi(q, \omega)$ is known. The rate at which these modes become occupied with increasing temperature enters in the transport properties and the exponent n in the power law of the resistivity $\rho(T) = \rho_0 + \tilde{A}T^n$ can be predicted. If the magnetic order occurs in three dimensions, $n = 3/2$ ($n = 5/3$ for

AFM (FM) order is predicted. Furthermore, the ordering temperature should depend on pressure as $T_N \propto (P_c - P)^{2/3}$ or as $T_C \propto (P_c - P)^{3/4}$.[38,39]

The theoretical predictions are in good agreement with the results presented in Sec. III B. The ordering temperature vanishes as $T_N \propto (P_c - P)^{0.71}$ and in the pressure range $P_c \pm 0.8$ GPa the electrical resistivity is described by $\rho(T) \propto T^n$ with $3/2 \leq n \leq 5/3$. Taken the similarity between CeRu$_2$Ge$_2$ and CeRu$_2$(Si$_{1-x}$Ge$_x$)$_2$ into account, AFM fluctuations might exist in CeRu$_2$Ge$_2$ close to the magnetic instability, leading to the exponent $n=1.5$ around P_c (see Fig. 6). The more this fluctuations are suppressed, i.e., tuning pressure towards 10 GPa, the more the FL properties dominate and the exponent approaches the FL state value ($n=2$).

The deviation from FL behavior in $\rho(T)$ in the temperature range 30 mK$<T_A<1.5$ K around P_c raises the question of whether a FL description is applicable below a certain temperature which is, in this case, enormously suppressed. As can be seen in the inset of Fig. 6, such a temperature limit might exist below 300 mK but measurements extended to much lower temperature than it was possible here are necessary to clarify this point. However, this is a challenging experimental task.

In the vicinity of P_c the temperature dependence of $\rho(T)$ unequivocally deviates from the T^2 dependence, predicted in the Fermi-liquid theory. Such a non-T^2 dependence of $\rho(T)$ was already observed for CePd$_2$Si$_2$ (Ref. 62) and CeNi$_2$Ge$_2$.[63,64] The non-Fermi-liquid (NFL) behavior, i.e., $\rho(T) \propto T^n$ with $n<2$, found in these compounds seems to depend strongly on the value of the residual resistivity ρ_0. A relatively large $\rho_0 = 20~\mu\Omega$ cm in CePd$_2$Si$_2$ yields $\rho(T) \propto T^2$ near P_c,[65] whereas $\rho(T) \propto T^{1.2}$ in a sample with $\rho_0 = 5~\mu\Omega$ cm was found.[62] In a high quality CeNi$_2$Ge$_2$ polycrystal ($\rho_0 = 0.3~\mu\Omega$ cm) $\rho(T)$ obeyed a $T^{1.37}$ power law at low temperature.[66] The residual resistivity in CeRu$_2$Ge$_2$ is also relatively small ($\rho_0 \approx 2~\mu\Omega$ cm) and a NFL behavior around P_c is detected. This suggests that disorder plays a key role in the appearance of NFL behavior in these (isostructural) materials.

V. CONCLUSION

The electrical resistivity $\rho(T)$ of CeRu$_2$Ge$_2$ was measured in the temperature range 30 mK$<T<300$ K for quasihydrostatic pressures up to 11 GPa. The ferromagnetic order is suppressed below $P=3.5$ GPa and a different magnetically ordered state exists up to 7.2 GPa below $T_L \approx 3$ K. At a critical pressure $P_c = 8.70(5)$ GPa the antiferromagnetic order vanishes as $T_N \propto (P_c - P)^m$, with $m=0.71(8)$. This value is in between the two critical exponents predicted for quantum phase transitions in itinerant Fermion systems. In a pressure range $P_c \pm 0.8$ GPa, the $\rho(T)$ dependence deviates from a Fermi-liquid description and is described by $\rho(T) \propto T^n$ with $3/2 \leq n \leq 5/3$. This might be attributed to AFM fluctuations. As the FL state is reached, these fluctuations are suppressed, and the exponent approaches the FL state value ($n=2$). The appearance of this non-Fermi-liquid behavior raises the question about the role of disorder in CeRu$_2$Ge$_2$ and isostructural materials. The magnetoresistivity measurements revealed hints for a complex magnetic phase diagram. Pronounced features at different magnetic fields B_a and B_c point to the possibility that magnetic phases analogue to CeRu$_2$(Si$_{0.9}$Ge$_{0.1}$)$_2$ exist also in CeRu$_2$Ge$_2$ in the pressure range $3.5<P<7.8$ GPa. A feature reminiscent of the metamagneticlike field B_M in CeRu$_2$Si$_2$ is found at $P=7.8$ GPa. The pressure and x variation of the ordering temperatures in CeRu$_2$Ge$_2$ and CeRu$_2$(Si$_{1-x}$Ge$_x$)$_2$ are transformed into a volume dependence. For both systems the (T,V) diagrams are quantitatively the same. This agreement shows that the unit-cell volume is the crucial parameter in this ternary Ce system. To clarify the complex magnetic order especially close to the magnetic instability region further experiments are necessary.

[1] J.-M. Mignot, A. Ponchet, P. Haen, F. Lapierre, and J. Flouquet, Phys. Rev. B **40**, 10 917 (1989).

[2] S. Kambe, H. Suderow, J. Flouquet, P. Haen, and P. Leay, Solid State Commun. **95**, 449 (1995); **96**, 175 (1995) (corrigendum).

[3] K. Kadowaki and S. B. Woods, Solid State Commun. **58**, 507 (1986).

[4] R. A. Fisher, C. Marcenat, N. E. Phillips, P. Haen, F. Lapierre, P. Lejay, J. Flouquet, and J. Voiron, J. Low Temp. Phys. **84**, 49 (1991).

[5] S. Raymond, S. Kambe, L. P. Regnault, J. Flouquet, and P. Lejay, Physica B (to be published).

[6] J. D. Thompson, Y. Uwatoko, T. Graf, M. F. Hundley, D. Mandrus, C. Godart, L. C. Gupta, P. C. Canfield, A. Migliori, and H. A. Borges, Physica B **199&200**, 589 (1994).

[7] H. Wilhelm and D. Jaccard, Solid State Commun. **106**, 239 (1998).

[8] M. J. Besnus, A. Essaihi, N. Hamdaoui, G. Fischer, J. P. Kappler, A. Meyer, J. Pierre, P. Haen, and P. Lejay, Physica B **171**, 350 (1991).

[9] A. Böhm, R. Caspary, U. Habel, L. Pawlak, A. Zuber, F. Steglich, and A. Loidl, J. Magn. Magn. Mater. **76&77**, 150 (1988).

[10] M. J. Besnus, J. P. Kappler, P. Lehmann, and A. Meyer, Solid State Commun. **55**, 779 (1985).

[11] J. Rossat-Mignod, L. P. Regnault, J. L. Jacoud, C. Vettier, P. Lejay, J. Flouquet, E. Walker, D. Jaccard, and A. Amato, J. Magn. Magn. Mater. **76&77**, 376 (1988).

[12] P. Haen, J. Flouquet, F. Lapierre, P. Lejay, and G. Remenyi, J. Low Temp. Phys. **67**, 391 (1987).

[13] S. Raymond, L.-P. Regnault, S. Kambe, J. M. Mignot, R. Lejay, and J. Flouquet, J. Low Temp. Phys. **109**, 205 (1997).

[14] P. Haen, F. Mallmann, M. J. Besnus, J. P. Kappler, F. Bourdarot, P. Burlet, and T. Fukuhara, J. Phys. Soc. Jpn. **65**, Suppl. B, 16 (1996).

[15] P. Haen, H. Bioud, and T. Fukuhara, Physica B (to be published).

[16] J.-M. Mignot, Ph. Boutrouille, L. P. Regnault, P. Haen, and P. Lejay, Solid State Commun. **77**, 317 (1991).

[17] J.-M. Mignot, J.-L. Jacoud, L. P. Regnault, J. Rossat-Mignod, P. Haen, P. Lejay, Ph. Boutrouille, B. Hennion, and D. Petitgrand, Physica B **163**, 611 (1990).

[18] S. Quezel, P. Burlet, J. L. Jacoud, L. P. Regnault, J. Rossat-Mignod, P. Lejay, and J. Flouquet, J. Magn. Magn. Mater. **76&77**, 403 (1988).

[19] T. C. Kobayashi, T. Miyazu, K. Shimizu, K. Amaya, Y. Kitaoka, Y. Ōnuki, M. Shirase, and T. Takabatake, Phys. Rev. B **57**, 5025 (1998).

[20] S. Süllow, M. C. Aronson, B. D. Rainford, and P. Haen, Physica B (to be published).

[21] B. Bireckhoven and J. Wittig, J. Phys. E **21**, 841 (1988).

[22] L. Spendeler, D. Jaccard, J. Sierro, M. François, A. Stepanov, and J. Voiron, J. Low Temp. Phys. **94**, 585 (1994).

[23] D. Jaccard, E. Vargoz, K. Alami-Yadri, and H. Wilhelm, Rev. High Pressure Sci. Technol. **7**, 412 (1998).

[24] A. Junod, in *Studies of High Temperature Superconductors*, edited by A. V. Narlikar (Nova Science, Commack, N.Y., 1996), Vol. 19. p. 1.

[25] B. Coqblin, in *The Electronic Structure of Rare-Earth Metals and Alloys: the Magnetic Heavy Rare-Earths*, edited by B. Coqblin (Academic, New York, 1977).

[26] R. Felten, G. Weber, and H. Rietschel, J. Magn. Magn. Mater. **63&64**, 383 (1987).

[27] B. Revaz, Ph.D.thesis, University of Geneva, 1998.

[28] Y. Uwatoko, G. Oomi, T. Graf, J. D. Thompson, P. C. Canfield, H. A. Borges, C. Godart, and L. C. Gupta, Physica B **206&207**, 234 (1995).

[29] P. Haen (private communication).

[30] A. Amato, Ph.D. thesis, University of Geneva, 1988.

[31] P. Link, D. Jaccard, and P. Lejay, Physica B **225**, 207 (1996).

[32] D. Jaccard, K. Behnia, and J. Sierro, Phys. Lett. A **163**, 475 (1992).

[33] A. Loidl, K. Knorr, G. Knopp, A. Krimmel, R. Caspary, A. Böhm, G. Sparn, C. Geibel, F. Steglich, and A. P. Murani, Phys. Rev. B **46**, 9341 (1992).

[34] B. D. Rainford, J. Dakin, and A. Severing, J. Magn. Magn. Mater. **108**, 119 (1992).

[35] S. Doniach, Physica B **91**, 231 (1977).

[36] H. A. Borges, J. D. Thompson, C. Godart, and L. C. Gupta, in *Theoretical and Experimental Aspects of Valence Fluctuations and Heavy Fermions*, edited by L. C. Gupta and S. K. Malik (Plenum, New York, 1987), p. 413.

[37] N. H. Andersen, in *Crystalline Field and Structural Effects in f-Electron Systems*, edited by J. E. Crow, R. P. Guertin, and T. W. Mihalisin (Plenum, New York, 1980), p. 373.

[38] T. Moriya and T. Takimoto, J. Phys. Soc. Jpn. **64**, 960 (1995).

[39] A. J. Millis, Phys. Rev. B **48**, 7183 (1993).

[40] J. D. Thompson, J. O. Willis, C. Godart, D. E. MacLaughlin, and L. C. Gupta, Solid State Commun. **56**, 169 (1985).

[41] K. Payer, P. Haen, J.-M. Laurant, J.-M. Mignot, and J. Flouquet, Physica B **186-188**, 503 (1993).

[42] P. Haen, J.-M.Laurant, K. Payer, and J.-M. Mignot, in *Transport and Thermal Properties of f-electron systems*, edited by G. Oomi *et al.* (Plenum, New York, 1993), p. 145.

[43] P. Haen, F. Lapierre, J. Voiron, and J. Flouquet, J. Phys. Soc. Jpn. **65**, 27 (1996).

[44] P. Haen, J. Voiron, F. Lapierre, J. Flouquet, and P. Lejay, Physica B **163**, 519 (1990).

[45] J.-M. Mignot, L. P. Regnault, J.-L. Jacoud, J. Rossat-Mignod, P. Haen, and P. Lejay, Physica B **171**, 357 (1991).

[46] P. Haen, J. Flouquet, F. Lapierre, P. Lejay, J.-M. Mignot, A. Ponchet, and J. Voiron, J. Magn. Magn. Mater. **63&64**, 320 (1987).

[47] R. Djerbi, F. Lapierre, P. Haen, and J.-M. Mignot, J. Magn. Magn. Mater. **76&77**, 265 (1988).

[48] C. Marcenat, R. A. Fisher, N. E. Phillips, and J. Flouquet, J. Magn. Magn. Mater. **76&77**, 115 (1988).

[49] P. Lehmann, Ph.D. thesis, University of Strasbourg, 1987.

[50] R. Mock, B. Hillebrands, H. Schmidt, G. Güntherodt, Z. Fisk, and A. Meyer, J. Magn. Magn. Mater. **47&48**, 312 (1985).

[51] I. L. Spain, F. Steglich, U. Rauchschwalbe, and H. D. Hochheimer, Physica B **139&140**, 449 (1986).

[52] F.D. Murnaghan, Proc. Natl. Acad. Sci. USA **30**, 244 (1944).

[53] L. P. Regnault, W. A. C. Erkelens, J. Rossat-Mignod, P. Lejay, and J. Flouquet, Phys. Rev. B **38**, 4481 (1988).

[54] L. P. Regnault, J.-L. Jacoud, J.-M. Mignot, J. Rossat-Mignod, C. Vettier, P. Lejay, and J. Flouquet, Physica B **163**, 606 (1990).

[55] J. L. Jacoud, L. P. Regnault, J. M. Mignod, J. Rossat-Mignod, J. Flouquet, and P. Lejay, J. Magn. Magn. Mater. **131-132**, 131 (1992).

[56] J. Dakin, G. Rapson, and B. D. Rainford, J. Magn. Magn. Mater. **108**, 117 (1992).

[57] B. D. Rainford, A. J. Neville, D. T. Adroja, S. J. Dakin, and A. P. Murani, Physica B **223&224**, 163 (1996).

[58] S. Kambe, S. Raymond, L.-P. Regnault, J. Flouquet, P. Lejay, and P. Haen, J. Phys. Soc. Jpn. **65**, 3294 (1996).

[59] J. R. Schrieffer and P. A. Wolff, Phys. Rev. B **149**, 491 (1966).

[60] W. A. Harrison and G. K. Straub, Phys. Rev. B **36**, 2695 (1987).

[61] S. Imada, M. Tsunekawa, T. Iwasaki, S. Suga, Y. Ōnuki, F. Iga, M. Kasaya, Y. Kawasaki, K. Ishida, Y. Kitaoka, and K. Asayama, J. Magn. Magn. Mater. **177-181**, 387 (1998).

[62] F. M. Grosche, S. R. Julian, N. D. Mathur, and G. G. Lonzarich, Physica B **223&224**, 50 (1996).

[63] S. J. S. Lister, F. M. Grosche, F. V. Carter, R. K. W. Haselwimmer, S. S. Saxena, N. D. Mathur, S. R. Julian, and G. G. Lonzarich, Z. Phys. B **103**, 263 (1997).

[64] F. Steglich, B. Buschinger, P. Gegenwart, M. Lohmann, R. Helfrich, C. Langhammer, P. Hellmann, L. Donnevert, S. Thomas, A. Link, C. Geibel, M. Lang, G. Sparn, and W. Assmus, J. Phys.: Condens. Matter **8**, 9909 (1996).

[65] P. Link, D. Jaccard, and P. Lejay, Physica B **223&224**, 303 (1996).

[66] F. Steglich, P. Gegenwart, R. Helfrich, C. Langhammer, P. Hellmann, L. Donnevert, C. Geibel, M. Lang, G. Sparn, W. Assmus, G. R. Stewart, and A. Ochiai, Z. Phys. B **103**, 235 (1997).